

# Hydrothermal ZnO Photocatalysis for Efficient Removal of Tetracycline from Wastewater

Wan Nuraishah Wan Ishak <sup>\*,1</sup>

Huey Ling Tan <sup>\*,1</sup>

Noor Fitrah Abu Bakar <sup>1</sup>

Ying Pei Lim <sup>1</sup>

Ng Law Yong <sup>2,3</sup>

Chun Yang Yin <sup>4</sup>

<sup>1</sup> School of Chemical Engineering, College of Engineering, Universiti Teknologi MARA, 40450, Shah Alam, Selangor, Malaysia

<sup>2</sup> Department of Chemical Engineering, Lee Kong Chian Faculty of Engineering and Science, Universiti Tunku Abdul Rahman, Jalan Sungai Long, Bandar Sungai Long, 43000, Kajang, Selangor, Malaysia

<sup>2</sup> Centre for Advanced and Sustainable Materials Research (CASMR), Universiti Tunku Abdul Rahman, Jalan Sungai Long, Bandar Sungai Long, 43000, Kajang, Selangor, Malaysia

<sup>4</sup> Newcastle University in Singapore, 537 Clementi Road #06-01, SIT Building @ Ngee Ann Polytechnic, Singapore 599493, Singapore

e-mail: aishahishak321@gmail.com (W.N.W.I); hueyling@uitm.edu.my (H.L.T)

*Submitted* 25 September 2024

*Revised* 8 April 2025

*Accepted* 10 April 2025

---

**Abstract.** Tetracycline (TC), a widely used antibiotic, is increasingly detected in wastewater, posing a significant environmental and health risk. Zinc oxide nanoparticles are emerging as a promising photocatalyst for TC photodegradation due to their low cost and superior light absorption capabilities at room temperature compared to the widely used titanium dioxide (TiO<sub>2</sub>). This study explores the efficacy of hydrothermally synthesized ZnO nanoparticles in degrading TC. The photocatalytic degradation efficiency of ZnO was examined under controlled batch conditions by varying parameters like ZnO dosage (0.5-2.5 g/L), TC concentration (5-25 ppm), and light source (solar, visible, and UV). The result showed that the highest TC removal efficiency (70.17%) was achieved under UV light with 1 g/L ZnO for a 5 ppm TC solution. The synthesized ZnO nanoparticles showed excellent reusability, highlighting their potential as a cost-effective and sustainable approach for TC degradation in wastewater treatment applications.

**Keywords:** Advanced Oxidation, Hydrothermal Reaction, Photocatalysis, Tetracycline, Zinc Oxide.

## INTRODUCTION

The global surge in pharmaceutical use has led to their unintended presence in aquatic environments. Antibiotics, a vital tool in human and animal healthcare, are a major

contributor to this growing problem. These drugs are increasingly recognized as emerging pollutants due to potential harm to human health and ecosystems (Bai *et al.*, 2022). Traditional wastewater treatment methods often struggle with antibiotics due

to their low biodegradability (Fiaz, *et al.*, 2021). This can lead to environmental and health risks, including the development of antibiotic resistance. Conventional methods like coagulation and biological systems can only remove 60-90% of antibiotics, leaving a significant portion behind (Bai *et al.*, 2022). In Malaysia, a study reported the detection of 23 antibiotics from six different classes in aquaculture farms, with tetracyclines showing the highest detection frequency at 83%. This highlights a significant environmental burden posed by tetracycline contamination in local aquatic systems and emphasizes the urgent need for effective removal strategies (Thiang *et al.*, 2021). Researchers are exploring various technologies for effective antibiotic removal from wastewater to address this challenge. These include adsorption, biodegradation, membrane filtration, ion exchange, and ozonation (Kraemer *et al.*, 2019). Among these, advanced oxidation processes (AOPs) stand out for their high efficiency and cost-effectiveness (Bai *et al.*, 2022). AOPs utilize powerful oxidants called hydroxyl radicals to break down and mineralize pollutants like tetracycline (TC) into simpler and harmless by-products, effectively removing them from the water. Photocatalysis is a specific type of AOPs that uses light to activate a semiconductor material (photocatalyst) that drives the degradation process (Bai *et al.*, 2022).

Common prominent photocatalysts used in wastewater treatment include titanium dioxide (TiO<sub>2</sub>), zinc oxide (ZnO), copper sulfides (CuS), and tin oxide (SnO<sub>2</sub>) (Aljaafari *et al.*, 2020). This research focuses on ZnO nanoparticles due to their remarkable reactivity, high photocatalytic activity, and ability to generate reactive oxygen species under light irradiation (Mousavi *et al.*, 2020). ZnO and TiO<sub>2</sub>, the most used semiconductors

in oxidation processes, have a band gap energy of about 3.2 eV, limiting their excitation to the ultraviolet (UV) radiation range (Rezaei *et al.*, 2021). However, ZnO nanoparticles are generally cheaper to produce than TiO<sub>2</sub> nanoparticles, and ZnO exhibits superior photon absorption efficiency at room temperature compared to TiO<sub>2</sub> under the same conditions. ZnO demonstrates versatility in degrading various pollutants, as shown by studies like Roy *et al.*, achieving 65 % degradation of methylene blue (MB) (Mousavi *et al.*, 2020). Similarly, (Rana *et al.*, 2017) synthesized Ni-doped ZnO and achieved near-complete degradation (98%) of norfloxacin, an antibiotic, within 120 minutes using a UV-A light source while Lv *et al.* investigated the photocatalytic activity of ZnO in degrading rhodamine B dye under both sunlight and UV radiation (Lv *et al.* 2011). The ZnO showed efficient photocatalytic activity, achieving nearly 90% dye degradation under UV irradiation. On the other hand, El Sharkawy *et al.* studied the use of photocatalysts N-TiO<sub>2</sub> for degrading organic pollutants in municipal wastewater (El Sharkawy *et al.*, 2023). Their findings demonstrated the effectiveness of these photocatalysts under both UV and solar radiation, achieving degradation levels exceeding 82 % [8]. However, a critical aspect of practical application is the reusability and regeneration of the ZnO photocatalyst. While ZnO offers advantages in cost and efficiency, its long-term performance and sustainability rely on the ability to reuse after the degradation process. Limited research explores the effectiveness of bare ZnO regeneration techniques and their impact on the catalyst's photocatalytic activity over multiple cycles. Investigating methods to regenerate ZnO and assess its performance over extended use will be crucial for

evaluating its economic and environmental feasibility in wastewater treatment. This study investigates the reusability and regeneration of ZnO as a photocatalyst for antibiotic degradation in wastewater treatment, demonstrating its potential as a more efficient and cost-effective approach due to its broad light absorption spectrum. By exploring the optimal parameters for ZnO-mediated degradation, we aim to evaluate its effectiveness and develop a more sustainable and efficient approach to addressing antibiotic contamination. In this work, ZnO nanoparticles were prepared using the hydrothermal method, using zinc acetate as the precursor due to its high yield and simple process. The as-prepared ZnO photocatalyst was characterized using various techniques such as X-ray diffraction (XRD), Fourier Transform Infrared (FTIR), Field Emission Scanning Electron Microscopy (FESEM), SEM-EDX and Ultraviolet-Diffuse Reflectance Spectroscopy (UV-DRS). ZnO's photocatalytic efficiency for removing tetracycline from wastewater was evaluated by varying ZnO loading, concentration of tetracycline, and light source.

## MATERIALS AND METHODS

### Materials

Zinc acetate dihydrate (98%), 0.8 M of sodium hydroxide (NaOH > 99%), and ethanol (95%) were acquired from R&M Chemicals. Tetracycline (TC > 95%) was purchased from Sigma Aldrich. All the chemicals used were of analytical grade and deionized (DI) water was used to prepare the solutions.

### Synthesis of ZnO Nanoparticles

The ZnO nanoparticles were synthesized using a hydrothermal method according to

Mukherjee *et al.* (2021) due to its ability to produce well-crystallized nanoparticles with controlled morphology at relatively low temperatures (80°C). This reduces energy consumption compared to high-temperature methods such as wet impregnation and chemical precipitation (Mukherjee *et al.*, 2021). Moreover, the hydrothermal approach eliminates the need for complex precursors or hazardous solvents, making it more environmentally friendly and scalable. In contrast, as reported by Ayu *et al.*, the synthesis of nitrogen doped ZnO typically requires high temperatures (~500°C) to incorporate nitrogen into the ZnO lattice, leading to significantly higher energy consumption. Given these considerations, the hydrothermal method was chosen for its superior crystallinity, controlled morphology, and enhanced sustainability in photocatalytic applications (Ayu *et al.*, 2023). Briefly, 0.3 g of zinc acetate was dissolved with constant stirring in 5 mL of deionized water. The solution's pH was then adjusted to 11 using 0.8 M NaOH. The resulting mixture was transferred to a Teflon-lined stainless-steel autoclave. The autoclave was placed in an oven (Mettler UF110) and heated at a controlled rate of 5°C/min until reaching 80°C, where it was maintained for 3 hours to ensure a complete reaction. After the reaction, the synthesized ZnO nanoparticles were recovered by centrifugation at 5,000 rpm for 15 minutes and dried overnight at 60°C.

### Characterization of ZnO Photocatalyst

The crystallinity of the ZnO nanoparticles was determined using a Rigaku Ultima IV XRD diffractometer. The analysis was performed in the  $2\theta$  range of 10–90° with Cu K $\alpha$  radiation ( $\lambda = 1.504 \text{ \AA}$ ) at a scan rate of 8 min<sup>-1</sup> and operating parameters of 40 kV and 30 mA.

Functional groups present in the ZnO nanoparticles were identified using FTIR spectroscopy. The analysis was conducted in the mid-infrared region in  $400\text{--}4000\text{ cm}^{-1}$ . Scanning Electron Microscopy (HITACHI SU3500 SEM) along with the attached Energy Dispersive X-ray (EDX, Oxford Instruments) with the voltage 15 kV and magnification of 5,000x to 10,000x was used to study the morphology and elemental composition of ZnO. The band gap energy of the ZnO nanoparticles was determined using Ultra-Violet Diffuse Reflectance Spectroscopy (UV-DRS Shimadzu 3600) equipped with a diffuse reflectance accessory (Cary 300-800). The UV-Vis absorption spectrum of the ZnO nanoparticles was obtained using a PerkinElmer Lambda 750 UV-Vis/NIR spectrophotometer. Barium sulfate ( $\text{BaSO}_4$ ) was used as a reference for the measurement.

### Photocatalytic Degradation of Tetracycline

The photocatalytic degradation of tetracycline (TC) using synthesized ZnO nanoparticles was investigated. Standard TC solutions (2–12 mg/L) were prepared via serial dilution from a stock solution (1000 mg/L) using deionized water for calibration. The photocatalytic activity was assessed by monitoring the degradation of a 5 mg/L TC solution (50 mL) with 0.05 g of ZnO under UV-C light (15 W, 10 cm distance) in a closed chamber (Figure 1). The mixture was stirred in the dark for 30 minutes to establish adsorption-desorption equilibrium, followed by 3 hours of UV irradiation. The experiment was repeated with different ZnO dosages (0.05–2.5 g/L), TC concentrations (5–25 mg/L), and light sources (solar, visible, UV) to assess the influence of various factors. The ZnO dosage variation explored the impact of catalyst loading while varying TC concentration assessed system capacity and

saturation points. Employing different light sources provided insights into degradation efficiency under various conditions (UV for benchmark, visible for realism, and solar for real-world applications). Control experiments were conducted to evaluate the contributions of photolysis (light irradiation without ZnO) and adsorption (mixing TC with ZnO in the dark) to the overall degradation process. The TC concentration in each sample was determined using a pre-generated standard curve, and the removal efficiency,  $E$ , was calculated using Eq. 1 (Xu *et al.*, 2023), where  $C_0(\text{mg/L})$  is the initial concentration of TC while  $C_t(\text{mg/L})$  is the final concentration of TC.

$$E = \frac{C_0 - C_t}{C_0} \times 100 \% \quad (1)$$

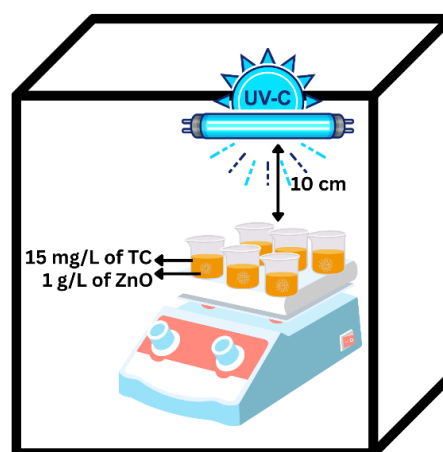


**Fig.1:** Schematic illustration of the photodegradation setup for tetracycline under UVC illumination

## RESULTS AND DISCUSSION

### Fourier Transform Infrared (FTIR)

Figure 2a presents the FTIR spectra of the samples. Absorption bands below  $1000\text{ cm}^{-1}$  correspond to interatomic vibrations within the ZnO nanoparticles. Characteristic peaks for Zn–O are observed at  $455\text{ cm}^{-1}$ ,  $941\text{ cm}^{-1}$ ,  $820\text{ cm}^{-1}$ , and  $680\text{ cm}^{-1}$ . The peak at  $1639$

$\text{cm}^{-1}$  indicates O-H bending vibrations, potentially from surface hydroxyl groups. A broad band centered at  $3415 \text{ cm}^{-1}$  is attributed to O-H stretching and bending modes, suggesting the presence of adsorbed water molecules on the samples. Additionally, the peak at  $1425 \text{ cm}^{-1}$  corresponds to the stretching vibrations of C-O-C groups. These observations are consistent with previous reports in the literature (Bashir *et al.*, 2022; Mukherjee *et al.*, 2021; Xu *et al.*, 2023).

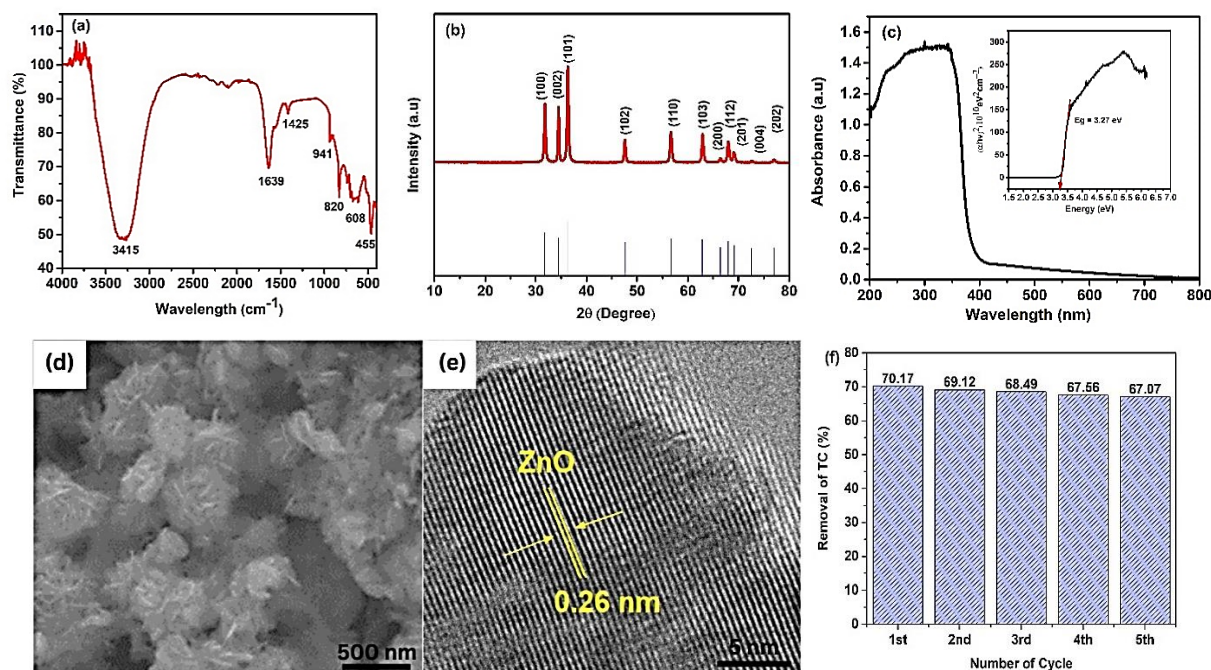
### X-ray Diffraction (XRD)

Figure 2b depicts the synthesized ZnO nanoparticles' X-ray diffraction (XRD) pattern. The diffraction peaks observed at  $31.8^\circ$ ,  $34.4^\circ$ ,  $36.3^\circ$ ,  $47.6^\circ$ ,  $56.6^\circ$ ,  $62.9^\circ$ ,  $66.5^\circ$ ,  $67.9^\circ$ ,  $69.1^\circ$ , and  $76.9^\circ$  correspond to the (100), (002), (101), (102), (110), (103), (200), (112), (201), and (202) planes of the wurtzite hexagonal phase of ZnO (JCPDS No. 36-1451), respectively. The most intense peak at  $36.3^\circ$

confirms the wurtzite structure (Ankamwar *et al.*, 2017). The Debye-Scherrer equation was employed to calculate the crystallite size using the peak corresponding to the (101) plane. The estimated crystallite size was  $30 \pm 10 \text{ nm}$ . This finding is consistent with similar XRD patterns reported in the literature for ZnO nanoparticles (Bashir *et al.*, 2022; Li *et al.*, 2013; Mukherjee *et al.*, 2021). The average crystallite size (D) of the ZnO nanoparticles was determined using the Debye-Scherrer formula, which is expressed as Eq. 2 (Ayu *et al.*, 2023):

$$D = \frac{0.9\lambda}{\beta \cos \theta} \quad (2)$$

where  $\lambda$  represents the wavelength of the incident X-ray ( $1.54 \text{ \AA}$ ),  $\beta$  denotes the full width at half maximum (FWHM), and  $\theta$  corresponds to the diffraction angle associated with the most intense peak of the (101) plane.



**Fig. 2:** (a) FTIR spectrum of the synthesized ZnO nanoparticles showing characteristic peaks corresponding to various functional groups; (b) XRD patterns of ZnO nanoparticles with (101) as the most intense peak; (c) Diffuse reflectance spectrum and plot of transferred Kubelka–Munk vs energy of the light absorbed for ZnO nanoparticles (inset); (d) SEM images and (e) HRTEM images of ZnO nanoparticles; (f) Re-usability of ZnO up to five cycles at 5 ppm of TC and  $1 \text{ gL}^{-1}$  of ZnO nanoparticles

### Scanning Electron Microscopy with Energy Dispersive X-ray and Transmission Electron Microscopy

SEM-EDX was performed for ZnO nanoparticles synthesized through a hydrothermal method, which appeared as white powders with fine crystalline structures (Figure 2d). ZnO nanoparticles exhibit flower-like structures with nanometric dimensions and slight agglomeration. This observed morphology is consistent with the findings of Ejsmont and Goscińska (Ejsmont and Goscińska, 2023). The elemental composition consisted of approximately 43.5 % (75.9 wt%) of zinc and 56.5 % (24.1 wt%) of oxygen, as shown in Table 1. This translates to a Zn:O atomic ratio of roughly 1:1.3, which closely aligns with the theoretical 1:1 ratio for ZnO reported by Malakootian *et al.* (Malakootian *et al.*, 2021). Notably, the observed higher oxygen content compared to zinc is to the previous findings for hydrothermally produced zinc oxide (Atchudan *et al.*, 2020). The lattice fringes of ZnO nanoparticles were observed to be 0.26 nm (Figure 2e) based on HRTEM analysis. This result aligns with other literature reporting ZnO fringes in the 0.26 – 0.29 nm (Li *et al.*, 2013; Mukherjee *et al.*, 2021).

**Table 1.** Weight and Atomic Percentage of the Element in ZnO nanoparticles

Element	Weight (%)	Atomic (%)
Zn	75.89	43.51
O	24.11	56.49
Total	100	

### Optical properties

The UV-visible spectra of the synthesized ZnO nanoparticle were run in the range of 300 to 800 nm, as shown in Figure 2c. The absorption peak of the ZnO nanoparticles was assigned to about 367 nm, comparable

with results reported by Baruah *et al.*, (Baruah *et al.*, 2009). The absorption peak obtained exhibited a blue shift, which could be attributed to quantum size effects and a decrease in size (Aljaafari *et al.*, 2020), due to low energy transitions and surface morphology changes. This observation is similar to the study conducted by Preethi *et al.*, who also reported that hydrothermal synthesis of ZnO leads to a blue shift in wavelength as compared to the sol-gel method (Baruah *et al.*, 2009). Generally, Bulk ZnO has a band gap range of 3.10 to 3.37 eV (Liang *et al.*, 2020). The band gap is estimated using the Tauc expression as shown in Eq. 3.

$$(\alpha h\nu)^2 = A (h\nu - E_g) \quad (3)$$

where  $\alpha$  ( $\text{cm}^{-1}$ ) is the absorption coefficient,  $A$  is the proportionality constant,  $h\nu$  (eV) is the incident light's frequency, and  $E$  (eV) is the band gap of the sample. From Figure 2(c) (inset), the intercept of the linear fit of Tauc's plot and extrapolation of the plot towards the x-axis gives  $E_g$ (bandgap). The band gap of ZnO nanoparticles synthesized through the hydrothermal method using zinc acetate as a precursor is approximately 3.27 eV, and it falls under the bulk ZnO band gap range.

### Effect of the ZnO Loading

The influence of catalyst loading on the photocatalytic degradation of tetracycline (TC) was investigated. ZnO nanoparticles were employed at varying concentrations (0.5 – 2.5 g/L) under UV light irradiation for 180 minutes (Figure 3a). The selected photocatalyst dosage range was determined based on performance evaluation and aligns with values commonly reported in wastewater studies (Saadati, Keramati, and Ghazi 2016). The photocatalytic efficiency initially increased with increasing ZnO loading, reaching a maximum removal



efficiency of 53.51% for 1.0 g/L of ZnO nanoparticles loading (Figure 3a). This enhancement can be attributed to the availability of a greater number of active sites on the catalyst surface at higher loadings. However, further increments in ZnO concentration resulted in a decrease in photocatalytic efficiency. This observation aligns with the findings of Malakootian *et al.*, who reported a similar decline in degradation beyond the optimal catalyst dosage (Malakootian *et al.*, 2021). Liang *et al.* suggested that excessive catalyst loading can hinder light penetration into the target solution due to light-scattering effects (Wu *et al.*, 2020). Consequently, the optimal ZnO loading for TC degradation under the employed conditions was 1.0 g/L. This finding revealed that the photocatalytic efficiency of ZnO nanoparticles synthesized hydrothermally in this study was slightly less than 5% lower than that of commercially available ZnO nanoparticles, which were 58.3 % (unpublished data).

### Effect of TC Concentration

The impact of initial TC concentration (5 – 25 ppm) on photocatalytic degradation was examined using 1 g/L ZnO under UV light irradiation (Figure 3b). After 180 minutes, the removal efficiency reached 70.17% for the 5 ppm TC solution. Conversely, a significantly lower removal efficiency of 19.76% was achieved for the 25 ppm TC solution. These observations are consistent with the findings reported by Mousavi *et al.* (Mousavi *et al.*, 2020). Generally, a decline in TC removal efficiency was observed with increasing TC concentration. This phenomenon can be attributed to the crucial role of active sites in photocatalysis. As the initial TC concentration increases, fewer active sites on the ZnO surface for TC adsorption are available. A

higher TC concentration reduces the light penetration depth within the solution due to increased light scattering.

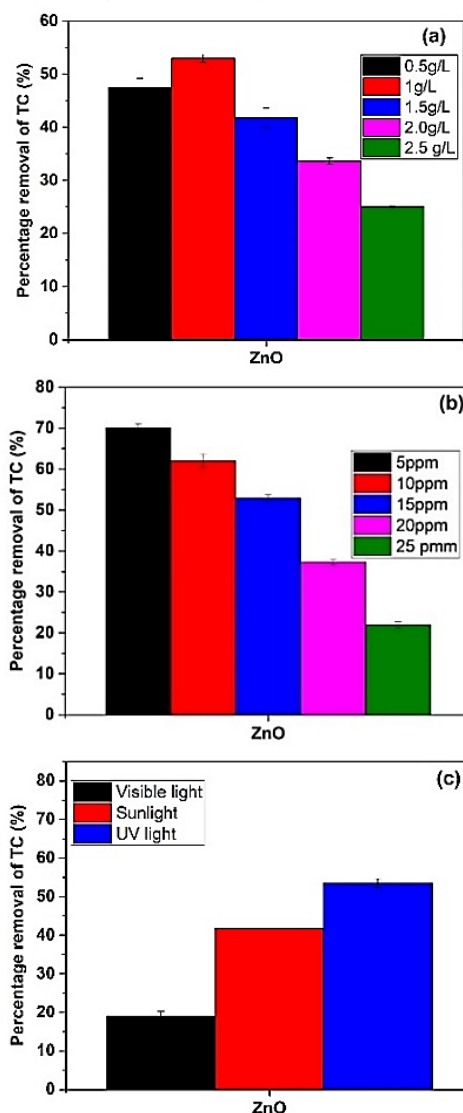


**Fig. 3:** Percentage removal of TC at (a) difference ZnO loading ( $C_0 = 15$  ppm of TC); (b) difference TC concentration ( $C_0 = 1\text{ g/L}^{-1}$  of ZnO nanoparticles); (c) difference light source ( $C_0 = 15$  ppm of TC,  $1\text{ g/L}^{-1}$  of ZnO nanoparticles under 180 min)

Consequently, the accumulation of TC on the ZnO surface hinders the generation of sufficient hydroxyl radicals, leading to a decrease in photocatalytic degradation efficiency (Malakootian *et al.*, 2021). This performance was comparable with ZnO nanoparticle commercial (data not

presented) and TiO<sub>2</sub> from a previous study. For example, Kouhail *et al.* (2020) reported that their synthesized TiO<sub>2</sub> achieved a 61% degradation of methylene blue at an optimal concentration of 5 ppm. In our study, the ZnO nanoparticles exhibited the highest performance at an optimal concentration of 5 ppm (Figure 3a). This suggests a comparable photocatalytic activity for both materials at this concentration. Furthermore, the ZnO synthesized in the present study exhibited superior performance, 8% higher compared to commercially available TiO<sub>2</sub> and ZnO nanoparticles, at 62.2% (unpublished data).

### Effect of Light Source on the Degradation of TC

The influence of the light source on TC degradation using ZnO was evaluated by employing three different sources: UV light, visible light, and sunlight. Experiments were conducted using 0.05 g ZnO with a 15 ppm TC solution for 180 minutes (Figure 3c). The highest removal efficiency (53.51%) was achieved under UV light irradiation, while the lowest (19.08%) was observed under visible light. These findings demonstrate that photocatalytic degradation of TC exhibits a significantly enhanced response when irradiated with UV light. This phenomenon can be attributed to the efficient photoactivation of the ZnO photocatalyst. Upon UV light absorption, electrons transition from the ZnO's valence band to the conduction band, generating holes in the valence band simultaneously. This process facilitates the reduction of oxygen molecules, forming superoxide radicals (O<sub>2</sub><sup>•−</sup>). Additionally, water molecules or OH<sup>−</sup> ions are oxidized, generating hydroxyl radicals (OH<sup>•</sup>) (Abejón *et al.*, 2015). Both superoxide and hydroxyl radicals play a crucial role in the degradation mechanism of TC. Conversely,

the limited photocatalytic activity observed under visible light can be attributed to insufficient activation of the ZnO band gap (Khan, Bae, and Jung 2010). This restricts generating a sufficient quantity of reactive species, particularly hydroxyl radicals (Gopal *et al.*, 2020). Our observations are consistent with the work of Saadhati *et al.*, who reported degradation rates exceeding 60% for an antibiotic under UV light irradiation with ZnO as the photocatalyst, followed by solar light, within a 180-minute time frame (Saadati *et al.*, 2016). This finding aligns with our UV-Vis diffuse reflectance spectroscopy (UV-DRS) results, which likely indicate a limited absorption of UV light by the synthesized ZnO. In addition, this result was comparable to commercially available ZnO nanoparticles at 58.3% (unpublished data) and TiO<sub>2</sub>, which ranges from 40-60% under UV light irradiation (Mohamed *et al.*, 2018). Our study shows the highest photodegradation compared to both photocatalysts. Table 2 compares the photocatalytic degradation efficiency of the ZnO nanoparticles synthesized in this study with recent reports on the degradation of various pollutants by TiO<sub>2</sub> and ZnO photocatalysts. This comparison highlights the promising potential of the ZnO nanoparticles synthesized in this study for the photocatalytic degradation of tetracycline from wastewater.

### Reusability of ZnO Nanoparticles

The reusability of the ZnO nanoparticles as a photocatalyst was evaluated by repeating the tetracycline (TC) degradation process for five cycles. Following each cycle, the photocatalyst was retrieved, washed with deionized (DI) water, and reused (Mukherjee *et al.*, 2021). The degradation profiles exhibited remarkable consistency across all



**Table 2.** Comparison of Photocatalytic Degradation Efficiency for Various Pollutants using TiO<sub>2</sub> and ZnO nanoparticles as Photocatalyst.

Photocatalyst	Light source	Initial Concentration (mg/L)	Degradation efficiency (%)	Reference
<b>TiO<sub>2</sub> nanoparticle</b>	UV lamp, 360 nm	10	25.1 % removal of TC under 120 min	(Wu <i>et al.</i> 2021)
<b>N-doped TiO<sub>2</sub> nanoparticles</b>	Xenon lamp, 400 nm	10	66.2 % removal of TC under 120 min	(Wu <i>et al.</i> 2021)
<b>TiO<sub>2</sub> nanoparticles</b>	Visible lamp, 400 nm	10	45 % removal of RhB dye under 210 min	(Gatou <i>et al.</i> 2023)
<b>TiO<sub>2</sub> zeolite</b>	UV lamp, 365 nm	10	12 % removal of Methyl Orange under 60 min	(Aziztyana <i>et al.</i> 2019)
<b>TiO<sub>2</sub> nanoparticles</b>	UV lamp, 365 nm	16	2 % removal of Methylene Blue under 150 min	(Zuo <i>et al.</i> 2014)
<b>ZnO NPs</b>	Natural sunlight	12	70 % removal of CIP under 110 min	(Mukherjee <i>et al.</i> 2021)
<b>ZnO nanoparticles</b>	Xe lamp, 420 nm	10	68 % removal of Sythetic Pigment under 30 min	(Xu <i>et al.</i> 2023)
<b>ZnO nanoparticles</b>	UV lamp, 365 nm	5	70.17 % removal of TC under 180 min	<b>This study</b>

cycles, as illustrated in Figure 2(f). Notably, the photocatalyst maintained a high level of efficacy, achieving a degradation rate of 67.07% for TC after 180 minutes in the fifth cycle. This represents a minimal decrease of approximately 3% compared to the initial cycle (70.17%). These findings demonstrate the exceptional stability and recyclability of the ZnO nanoparticles, signifying their potential for deployment in practical wastewater treatment applications due to the economic and environmental advantages associated with catalyst reusability.

### Cost and Scalability

This study evaluates the economic viability of a novel method for degrading tetracycline (TC) in wastewater. The proposed approach leverages ultraviolet (UV) light irradiation in combination with recyclable zinc oxide (ZnO) nanoparticles (Figure 4). The treatment system prioritizes simplicity, employing a single-unit centrifugal pump, a

photocatalytic reaction tank (2.3 m<sup>3</sup>/hr), a filtration unit, and six UV light sources. Wastewater containing TC and a pre-determined concentration (1000 mg/L) of ZnO nanoparticles are pumped into the reaction tank. The UV light exposure is meticulously controlled to achieve optimal degradation efficiency. Finally, a filtration unit efficiently recovers the ZnO nanoparticles for subsequent reuse. A comprehensive cost analysis revealed a treatment cost of approximately \$10.19/m<sup>3</sup> for achieving a 70% removal rate of TC. This dependence on raw material prices necessitates further investigation to mitigate potential cost fluctuations in the future. For comparison, a widely employed method for antibiotic removal, a flatbed reactor, incurs a substantially higher cost of \$903.16/m<sup>3</sup>, as reported by Duran *et al.* (2018) and in the range of \$70.0 and \$46.5 per m<sup>3</sup> for antibiotic removal (Ribeiro *et al.*, 2020). Considering the simpler design and significantly lower

operational costs, TC degradation using recyclable ZnO nanoparticles with UV light irradiation presents a promising alternative. The reusability of the ZnO nanoparticles further enhances the economic viability of this method.

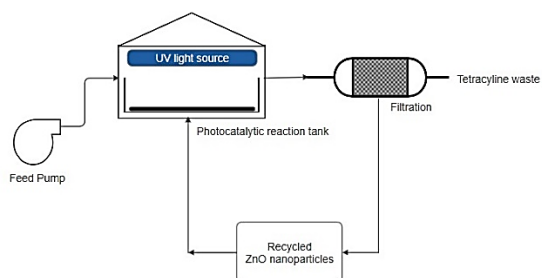


**Fig. 4:** Process flow diagram photocatalysis of ZnO nanoparticles

**Table 3.** Cost analysis for the proposed pilot scale photocatalytic process

Cost Component	Cost (\$)/m <sup>3a</sup>
Capital Costs over 10 years	
Photocatalytic Reaction Tank <sup>b</sup>	\$0.72
UV Light Source	\$0.14
Ultrafiltration Unit <sup>b</sup> (McGraw-Hill 1984)	\$0.34
Feed Pump <sup>b</sup>	\$0.074
Recycling System	\$0.22
Total Capital Cost	\$1.45
Operational Costs	
Energy Consumption (UV light source: 5 kW, feed pump: 2 kW, filtration: 2 kW, recycling system: 1 kW; \$0.10/kWh) <sup>c</sup>	\$0.44
Raw Material Cost <sup>f</sup>	\$0.05
Labor Cost <sup>e</sup>	\$4.35
Maintenance Cost (\$50/day) <sup>d</sup>	\$2.17
Waste Disposal Cost (\$20/day)	\$0.87
Utility Costs (\$30/day)	\$1.30
Total Operational Cost	\$8.74
Total Cost (per hour)	\$10.19

<sup>a</sup>The estimated annual cost of tetracycline (TC) removal is based on a batch wastewater treatment process that operated 10 hr/day, 6 days/week and 50 weeks/year.

<sup>b</sup>The estimated data of equipment is calculated based on data established by Perry of Chemical

Engineering Book, (Perry, 2008)

<sup>c</sup>The estimated cost is calculated using the Malaysian tariff rate established by Tenaga Nasional Berhad, (Tenaga Nasional Berhad, 2024)

<sup>d</sup>Based on cost for installation of TC removal using filtration

<sup>e</sup>The estimated cost incorporates 2024 Malaysian labour rates, (Indeed, 2024)

<sup>f</sup>The estimated cost of precursor material for ZnO synthesis is based on prices listed on the Sigma-Aldrich website, (Merck, 2024)

## CONCLUSION

In summary, hydrothermal synthesis successfully produced flower-like ZnO nanostructures with a crystallite size of  $30 \pm 10$  nm, a 3.27 eV band gap, and slight agglomeration. These ZnO nanoparticles exhibited superior photocatalytic activity for tetracycline degradation (70.17% under UV light within 180 minutes using 1 g/L) compared to commercially available TiO<sub>2</sub> and ZnO. Notably, the synthesized ZnO nanoparticles also demonstrated high stability and reusability, further highlighting its potential as a sustainable solution for antibiotic removal in wastewater treatment. The demonstrated efficiency, non-toxicity, stability, reusability, and cost-effectiveness of hydrothermally synthesized ZnO make it a promising candidate for real-world applications. However, further research is necessary to enhance the visible light activity of the ZnO photocatalyst. An intriguing avenue for future exploration lies in combining ZnO with other semiconductors to create composite photocatalysts. Tailoring these composites' band gaps and interfacial properties could lead to significantly improved performance and broader light absorption capabilities. This approach could ultimately lead to developing photocatalysts with optimal activity under diverse light conditions encountered in wastewater treatment facilities.

## ACKNOWLEDGMENT

This work was financially supported by the Ministry of Higher Education (MOHE) through the Fundamental Research Grant Scheme (FRGS/1/2022/TK0/UITM/02/39). The authors also thank the College of Engineering at Universiti Teknologi, MARA, for their assistance in completing the research project.

## REFERENCES

- Abejon, R., Cazes, M. De., Belleville, M. P., Sanchez-Marcano, J., 2015. "Large-scale enzymatic membrane reactors for tetracycline degradation in WWTP effluents." *Water Res.* 15(73), 118–131. <https://doi.org/10.1016/j.watres.2015.01.012>.
- Aljaafari, A., Ahmed, F., Awada, C., and Shaalan, N. M., 2020. "Flower-like ZnO nanorods synthesized by microwave-assisted one-pot method for detecting reducing gases: Structural properties and sensing reversibility." *Front. Chem.* 8, 456. <https://doi.org/10.3389/fchem.2020.00456>
- Ankamwar, B. G., Kamble, V. B., Annsi, J. I., Sarma, L. S., and Mahajan, C. M., 2017. "Solar photocatalytic degradation of methylene blue by ZnO nanoparticles." *J. Nanosci. Nanotechnol.* 17(2), 1185–1192. <https://doi.org/10.1166/jnn.2017.12579>
- Atchudan, R., Edison, T. N. J. I., Mani, S., Perumal, S., Vinodh, R., Thirunavukkarasu, S. and Lee, Y. R., 2020. "Facile synthesis of a novel nitrogen-doped carbon dot adorned zinc oxide composite for photodegradation of methylene blue." *Dalton Trans.* 49(48), 17725–17736. <https://doi.org/10.1039/d0dt02756a>
- Ayu, D. G., Gea, S., Andriyani, N., Telaumbanua, D. J., Piliang, A. F. R., Harahap, M., Yen, Z., Goei, R., and Yoong Tok, A. I., 2023. "Photocatalytic degradation of methylene blue using N-doped ZnO/carbon dot (N-ZnO/CD) nanocomposites derived from organic soybean." *ACS Omega* 8(17), 14965–14984. <https://doi.org/10.1021/acsomega.2c07546>
- Aziztyana, A. P., Wardhani, S., Prananto, Y. P., Purwonugroho, D., and Darjito, 2019. "Optimisation of Methyl Orange Photodegradation Using TiO<sub>2</sub>-Zeolite Photocatalyst and H<sub>2</sub>O<sub>2</sub> in acid condition." *IOP Conf. Ser. Mater. Sci. Eng.* 546(4), 042047. <https://doi.org/10.1088/1757-899X/546/4/042047>
- Bai, X., Chen, W., Wang, B., Sun, T., Wu, B., and Wang, Y., 2022. "Photocatalytic degradation of some typical antibiotics: Recent advances and future outlooks." *Int. J. Mol. Sci.* 23(15), 8130. <https://doi.org/10.3390/ijms23158130>
- Baruah, S., and Dutta, J., 2009. "Hydrothermal growth of ZnO nanostructures." *Sci. Technol. Adv. Mater.* 10(1). <https://doi.org/10.1088/1468-6996/10/1/013001>
- Bashir, S., Awan, M. S., Farrukh, M. A., Naidu, R., Khan, S. A., Rafique, N., Ali, S., Hayat, I., Hussain, I., and Khan, M. Z., 2022. "In-vivo (albino mice) and in-vitro assimilation and toxicity of zinc oxide nanoparticles in food materials." *Int. J. Nanomedicine* 17, 4073–4085. <https://doi.org/10.2147/IJN.S372343>
- Durán, A., Monteagudo, J. M., and Martín, I. S., 2018. "Operation costs of the solar photo-catalytic degradation of

- 
- pharmaceuticals in water: A mini-review." *Chemosphere* 211, 482–488. <https://doi.org/10.1016/j.chemosphere.2018.07.170>
- Ejsmont, A., and Goscińska, J., 2023. "Morphology controlled nitrogen-doped mesoporous carbon vehicles for sustained release of paracetamol." *Micropor. Mesopor. Mater.* 350, 112449. <https://doi.org/10.1016/j.micromeso.2023.112449>
- Fiaz, A., Zhu, D., and Sun, J., 2021. "Environmental fate of tetracycline antibiotics: Degradation pathway mechanisms, challenges, and perspectives." *Environ. Sci. Eur.* 33(1), 64.
- Gatou, M. A., Fiorentis, E., Lagopati, N., and Pavlatou, E. A., 2023. "Photodegradation of rhodamine b and phenol using TiO<sub>2</sub>/SiO<sub>2</sub> composite nanoparticles: a comparative study." *Water* 15(15), 2773. <https://doi.org/10.3390/w15152773>
- Gopal, G., Alex, S. A., Chandrasekaran, N., and Mukherjee, A., 2020. "A Review on tetracycline removal from aqueous systems by advanced treatment techniques." *RSC Adv.* 10(45), 27081–27095.
- Indeed. 2024. "Operators Salary in Malaysia." Retrieved July 14, 2024 (<https://malaysia.indeed.com/career/operator/salaries>).
- Khan, M. H., Bae, H., and Jung, J. Y., 2010. "Tetracycline degradation by ozonation in the aqueous phase: Proposed degradation intermediates and pathway." *J. Hazard., Mater.* 181(1–3), 659–665. <https://doi.org/10.1016/j.jhazmat.2010.05.063>
- Kouhail, M., Elberouhi, K., Elahmadi, Z., Benayada, A., and Gmouh, S., 2020. "A comparative study between TiO<sub>2</sub> and ZnO photocatalysis: Photocatalytic degradation of textile dye." *IOP Conf. Ser. Mater. Sci. Eng.* 827. <https://doi.org/10.1088/1757-899X/827/1/012009>
- Kraemer, S. A., Ramachandran A., and Perron, G. G., 2019. "Antibiotic pollution in the environment: From microbial ecology to public policy." *Microorganisms* 7(6), 180. <https://doi.org/10.3390/microorganisms7060180>
- Li, Y., Zhang, B. P., Zhao J. X., Ge Z. H., Zhao, X. K., and Zou, L., 2013. "ZnO/carbon quantum dots heterostructure with enhanced photocatalytic properties." *Appl. Surf. Sci.* 279, 367–373. <https://doi.org/10.1016/j.apsusc.2013.04.114>
- Liang, H., Tai, X., Du, Z., and Yin, Y., 2020. "Enhanced photocatalytic activity of ZnO Sensitized by carbon quantum dots and application in phenol wastewater." *Opti. Mater.* 100(26), 109674. <https://doi.org/10.1016/j.optmat.2020.109674>
- Lv, T., Pan, L., Liu, X., Lu, T., Zhu, G., and Sun, Z., 2011. "Enhanced photocatalytic degradation of methylene blue by ZnO-reduced graphene oxide composite synthesized via microwave-assisted reaction." *J. Alloys Compd.* 509(41), 10086–10091. <https://doi.org/10.1016/j.jallcom.2011.08.045>
- Malakootian, M., Asadzadeh, S. N., Mehdipoor, M., and Kalantar-Neyestanaki, D., 2021. "A new approach in photocatalytic degradation of tetracycline using biogenic zinc oxide nanoparticles and peroxy monosulfate under UVC irradiation." *Desal. Water Treat.* 222, 302–312.
-

- 
- <https://doi.org/10.5004/dwt.2021.27077>
- McGraw-Hill. 1984. *Perry's Chemical Engineers' Handbook*.
- Merck. 2024. "Sigma." Retrieved July 14, 2024 (<https://www.sigmaaldrich.com/MY/en>).
- Mohamed, R. M., Ismail, A. A., Kadi, M. W., and Bahnemann. D. W., 2018. "A comparative study on mesoporous and commercial TiO<sub>2</sub> photocatalysts for photodegradation of organic pollutants." *J. Photochem. Photobiol. A: Chemistry* 367, 66–73. <https://doi.org/10.1016/j.jphotochem.2018.08.019>
- Mousavi, S. B., and Heris, S. Z., 2020. "Experimental investigation of ZnO nanoparticles effects on thermophysical and tribological properties of diesel oil." *Int. J. Hydrogen Energy* 45(43), 23603–23614. <https://doi.org/10.1016/j.ijhydene.2020.05.259>
- Mukherjee, I., Cilamkoti, V., and Dutta, R. K., 2021. "Sunlight-driven photocatalytic degradation of ciprofloxacin by carbon dots embedded in ZnO nanostructures." *ACS Appl. Nano Mater.* 4(8), 7686–7697. <https://doi.org/10.1021/acsanm.1c00883>
- Perry, R. H., & Green, D. W., 2008. *Perry's Chemical Engineers' Handbook*. McGraw-Hill Education
- Rana, A. K., Kumar, Y., Rajput, P., Jha, S. N., Bhattacharyya, D., and Shirage, P. M., 2017. "Search for origin of room temperature ferromagnetism properties in Ni-doped ZnO nanostructure." *ACS Appl. Mater. & Interfaces* 9(8), 7691–7700. <https://doi.org/10.1021/acsami.6b12616>
- Rezaei, S. S., Kakavandi, B., Noorisepehr, M., Isari, A. A., Zabih, S., and Bashardoust, P., 2021. "Photocatalytic oxidation of tetracycline by magnetic carbon-supported TiO<sub>2</sub> nanoparticles catalyzed peroxydisulfate: Performance, synergy and reaction mechanism studies." *Sep. Purif. Technol.* 258, 117936. <https://doi.org/10.1016/j.seppur.2020.117936>
- Ribeiro, J. P., Marques, C. C., Portugal, I., and Nunes, M. I., 2020. "Fenton processes for AOX removal from a kraft pulp bleaching industrial wastewater: optimisation of operating conditions and cost assessment." *J. Environ. Chem. Eng.* 8(4), 104032. <https://doi.org/10.1016/j.jece.2020.104032>
- Saadati, F., Keramati, N., and Ghazi, M. M., 2016. "Influence of parameters on the photocatalytic degradation of tetracycline in wastewater: A review." *Crit. Rev. Environ. Sci. Technol.* 46(8), 1–26. <https://doi.org/10.1080/10643389.2016.1159093>
- Sharkawy, H. M., Shawky, A. M., Elshypany, R., and Selim H., 2023. "Efficient photocatalytic degradation of organic pollutants over TiO<sub>2</sub> nanoparticles modified with nitrogen and MoS<sub>2</sub> under visible light irradiation." *Sci. Rep.* 13(1), 8845. <https://doi.org/10.1038/s41598-023-35265-7>
- Tenaga Nasional, Industrial Tariffs. 2024. "Tenaga Nasional, Industrial Tariffs." Retrieved July 14, 2024 (<https://www.tnb.com.my/commercial-industrial/pricing-tariffs1>).
- Thiang, E. L., Lee, C. W., Takada, H., Seki, K., Takei, A., Suzuki, S., Wang, A., and Bong C. W., 2021. "Antibiotic residues from aquaculture farms and their ecological risks in Southeast Asia: A case study from Malaysia." *Ecosyst. Health Sustain.* 7(1), 1926337. <https://doi.org/10.1080/20964129.2021.1926337>
-

---

1926337

Wu, S., Hu, H., Lin, Y., Zhang, J., and Hu, Y. H., 2020. "Visible light photocatalytic degradation of tetracycline over  $\text{TiO}_2$ ." *Chem. Eng. J.* 382, 122842.

<https://doi.org/10.1016/j.cej.2019.122842>

Wu, S., Li, X., Tian, Y., Lin, Y., and Hu, Y. H., 2021. "Excellent photocatalytic degradation of tetracycline over black anatase- $\text{TiO}_2$  under visible light." *Chem. Eng. J.* 406, 126747.

<https://doi.org/10.1016/j.cej.2020.126747>

Xu, J. J., Lu, Y. N., Tao, F. F., Liang, P. F., and Zhang, P. A., 2023. "ZnO nanoparticles modified by carbon quantum dots for the photocatalytic removal of synthetic pigment pollutants." *ACS Omega* 8(8), 7845–7857.

<https://doi.org/10.1021/acsomega.2c07591>

Zuo, R., Du, G., Zhang, W., Liu, L., Liu, Y., Mei, L., and Li, Z., 2014. "Photocatalytic degradation of methylene blue using  $\text{TiO}_2$  impregnated diatomite." *Adv. Mater. Sci. Eng.* 2014(1), 170148.

<https://doi.org/10.1155/2014/170148>

---